

Outage probability analysis of EH NOMA system network over Rayleigh fading channel using selection combining at the receiver

Phu Tran Tin¹, Minh Tran², Tran Thanh Trang³

¹Faculty of Electronics Technology, Industrial University of Ho Chi Minh City, Vietnam

²Optoelectronics Research Group, Faculty of Electrical and Electronics Engineering,
Ton Duc Thang University, Vietnam

³National Key Laboratory of Digital Control and System Engineering, Vietnam

Article Info

Article history:

Received Jun 4, 2019

Revised Sep 26, 2019

Accepted Nov 10, 2019

Keywords:

Energy harvesting (EH)

Monte carlo

Outage probability (OP)

Power beacon

Relaying network

ABSTRACT

Non-orthogonal multiple access (NOMA) with advantages such as superior spectral efficiency has been considered as a promising multiple access technique for the fifth-generation (5G) mobile networks. In this research, we propose energy harvesting (EH) NOMA system relaying network over Rayleigh fading channel using selection combining at the receiver. Firstly, we investigate the system performance in terms of the closed-form expression of the outage probability (OP). Here we compare the OP of two destination users of the proposed system. Finally, all the results is convinced by the Monte Carlo simulation. From the results, we can confirm that all the analytical and simulation results are the same in connection with the primary system parameters.

This is an open access article under the [CC BY-SA](https://creativecommons.org/licenses/by-sa/4.0/) license.



Corresponding Author:

Minh Tran,

Optoelectronics Research Group,

Faculty of Electrical and Electronics Engineering,

Ton Duc Thang University, Ho Chi Minh City, Vietnam.

Email: tranhoangquangminh@tdtu.edu.vn

1. INTRODUCTION

Non-orthogonal multiple access (NOMA) with advantages such as superior spectral efficiency has been considered as a promising multiple access technique for the fifth-generation (5G) mobile networks [1-6]. In comparison with the traditional water-filling power allocation strategy, NOMA can transfer more power to the users in the worse channel conditions. It leads to a better trade-off between system throughput and user fairness. From the previous researches, authors investigated the impact of user pairing on downlink NOMA systems as in [7], the authors in [8] have considered the power allocation with the max-min fairness criterion of the model system. An uplink NOMA scheme with joint power and subcarrier allocations has been proposed and investigated in [9]. In [10], a cooperation-based NOMA scheme for coordinated direct and relay transmissions is studied. Furthermore, a diversity-oriented detection mechanism for the cooperative relaying system using NOMA is considered by authors in [11]. The performance of transmit antenna selection for NOMA assisted multiple-input-multiple-output (MIMO) relay networks is presented in [12]. Then inspired by user collaboration, a cooperative NOMA transmission scheme is presented in [13].

In this research, we propose energy harvesting (EH) NOMA network system over the Rayleigh fading channel using selection combining at the receiver. In the first stage, we investigate and derive

the closed-form expression of the outage probability (OP) of the model system by Monte Carlo simulation. Then the comparison of the OP of two destination users is investigated in connection with the primary system parameters. Finally, all the results are convinced by the Monte Carlo simulation. From the results, we can convince that all the analytical and simulation results are the same in connection with the primary system parameters. The main contributions of this research are listed as:

- The EH NOMA network system over the Rayleigh fading channel using selection combining at the receiver is proposed.
- The closed-form expression of the system OP is investigated and derived.
- The comparison of the OP of two destination users is investigated.
- All the results are convinced by the Monte Carlo simulation.

2. SYSTEM MODEL

The EH NOMA network system over the Rayleigh fading channel using selection combining at the receiver is drawn in Figure 1. In this system model, we denote Source is S, Relay is R, D₁ and D₂ are two Destination nodes. We assume that all links between them (i.e., S-to-D_{1,2}, S-to-R, and R-to-D_{1,2}) are available. The Rayleigh fading channel coefficients of S-to-D_{1,2}, S-to-R, and R-to-D_{1,2} links are denoted as h_{SD1,2}, h_{SR}, and h_{RD1,2}, respectively as shown in Figure 1. The energy harvesting and information processing (IT) are illustrated in Figure 2. In this protocol, the transmission block time T, which consists of three-time slots. In the first-time slot αT (α is the time switching factor, 0<α<1), the relay harvests energy from the source node S. In the second interval time (1-α)T/2, the source S transfers the information to R and D_{1,2} at the same time. Finally, the relay node R transfers the information to the destination nodes D_{1,2} in the remaining time slot (1-α)T/2.

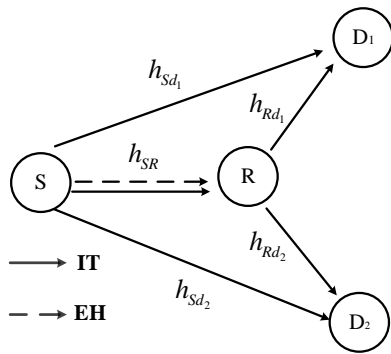


Figure 1. System model

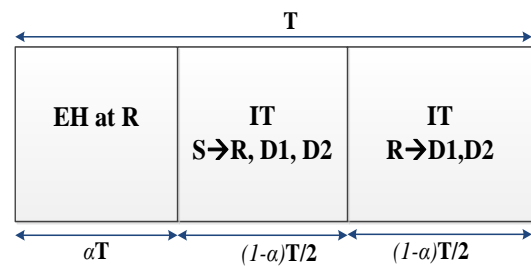


Figure 2. The time switching protocol

Energy harvesting phase

In the first slot time αT, we formulate the received signal as:

$$y_r = h_{sr} \sqrt{P_s} x_s + n_r \tag{1}$$

The received energy can be computed as:

$$E_r = \eta \alpha T |h_{sr}|^2 P_s \tag{2}$$

Where 0 < η < 1 is the energy conversion efficiency.

The average transmit power at the R node can be calculated as:

$$P_r = \frac{E_s}{(1-\alpha)T/2} = \kappa |h_{sr}|^2 P_s \tag{3}$$

Where we denote $\kappa = \frac{2\eta\alpha}{1-\alpha}$.

Information transmission

In the second slot time, S transmits the superposed signal $\sqrt{a_1 P_s} x_1 + \sqrt{a_2 P_s} x_2$ to relay, D₁ and D₂ according to the NOMA scheme [1]. a_1, a_2 are the power allocation coefficients for D₁ and D₂, where we assume $a_1 + a_2 = 1, a_2 > a_1$, x_1 and x_2 are the transmit signal for D₁ and D₂, respectively. Hence, the received signal at the R node, D₁ and D₂ can be expressed as respectively [14].

$$y_r = h_{sr} \left(\sqrt{a_1 P_s} x_1 + \sqrt{a_2 P_s} x_2 \right) + n_r \quad (4)$$

$$y_{D_1} = h_{sd_1} \left(\sqrt{a_1 P_s} x_1 + \sqrt{a_2 P_s} x_2 \right) + n_{d_1} \quad (5)$$

$$y_{D_2} = h_{sd_2} \left(\sqrt{a_1 P_s} x_1 + \sqrt{a_2 P_s} x_2 \right) + n_{d_2} \quad (6)$$

Where n_{d_1}, n_{d_2} are the additive white Gaussian noise (AWGN) at the D₁ and D₂ with zero-mean and variance N_0 , respectively. From (6), we separate the received signal at the D₂ into two parts included signal and noise part for D₂ to detect x_1 .

$$y_{D_2} = \underbrace{h_{sd_2} \sqrt{a_2 P_s} x_2}_{\text{signal}} + \underbrace{h_{sd_2} \sqrt{a_1 P_s} x_1 + n_{d_2}}_{\text{noise}} \quad (7)$$

Hence, the received signal to interference and noise ratio (SINR) for D₂ to detect x_1 is given as:

$$\gamma_{sd_2} = \frac{E\{|signal|^2\}}{E\{|noise|^2\}} = \frac{|h_{sd_2}|^2 a_2 P_s}{|h_{sd_2}|^2 a_1 P_s + N_0} = \frac{|h_{sd_2}|^2 a_2 \psi}{|h_{sd_2}|^2 a_1 \psi + 1} \quad (8)$$

Where $\psi = \frac{P_s}{N_0}$ is the transmit signal to noise ratio (SNR).

From (5), SIC is first used for D₁ by detecting and decoding the information of D₂. Hence, the received signal at the D₁ can be rewritten as:

$$y_{D_1} = \underbrace{h_{sd_1} \sqrt{a_2 P_s} x_2}_{\text{signal}} + \underbrace{h_{sd_1} \sqrt{a_1 P_s} x_1 + n_{d_1}}_{\text{noise}} \quad (9)$$

Then, the received SINR at D₁ is given by:

$$\gamma_{sd_1} = \frac{|h_{sd_1}|^2 a_2 \psi}{|h_{sd_1}|^2 a_1 \psi + 1} \quad (10)$$

After the far user message is decoded, D₁ can decode its own information with the SINR as following

$$\gamma_{sd_1} = |h_{sd_1}|^2 a_1 \psi \quad (11)$$

During the third slot time, the relaying node will amplify the received signal and forward to D₁ and D₂ with the amplifying factor $\beta = \frac{x_r}{y_r} = \sqrt{\frac{P_r}{P_s |h_{sr}|^2 + N_0}}$. The received signals at the D₁ and D₂ are expressed as, respectively.

$$y_{rd_1} = h_{rd_1} x_r + n_{rd_1} = h_{rd_1} \beta y_r + n_{rd_1} \tag{12}$$

Substituting (4) into (12)

$$y_{rd_1} = h_{rd_1} \beta \left[h_{sr} \left(\sqrt{a_1 P_s} x_1 + \sqrt{a_2 P_s} x_2 \right) + n_r \right] + n_{rd_1} \tag{13}$$

And

$$\begin{aligned} y_{rd_2} &= h_{rd_2} x_r + n_{rd_2} = h_{rd_2} \beta y_r + n_{rd_2} \\ &= h_{rd_2} h_{sr} \beta \left(\sqrt{a_1 P_s} x_1 + \sqrt{a_2 P_s} x_2 \right) + h_{rd_2} \beta n_r + n_{rd_2} \end{aligned} \tag{14}$$

Where n_{rd_1}, n_{rd_2} was denoted the AWGN at D1 and D2, respectively. From (14), the received SINR for D2 to detect x_2 is given as:

$$\gamma_{rd_2} = \frac{E\{|signal|^2\}}{E\{|noise|^2\}} = \frac{|h_{sr}|^2 |h_{rd_2}|^2 a_2 \psi}{|h_{sr}|^2 |h_{rd_2}|^2 a_1 \psi + |h_{rd_2}|^2 + 1/\beta^2} \tag{15}$$

Using the fact that $N_0 \ll P_r$, hence, (15) can be rewritten as:

$$\begin{aligned} \gamma_{rd_2} &= \frac{|h_{sr}|^2 |h_{rd_2}|^2 a_2 \psi}{|h_{sr}|^2 |h_{rd_2}|^2 a_1 \psi + |h_{rd_2}|^2 + 1/\beta^2} \\ &\approx \frac{|h_{sr}|^2 |h_{rd_2}|^2 a_2 \psi}{|h_{sr}|^2 |h_{rd_2}|^2 a_1 \psi + |h_{rd_2}|^2 + 1/\kappa} \end{aligned} \tag{16}$$

The received SINR when D1 first detect D2's information is given by:

$$\gamma_{rd_{21}} \approx \frac{|h_{sr}|^2 |h_{rd_1}|^2 a_2 \psi}{|h_{sr}|^2 |h_{rd_1}|^2 a_1 \psi + |h_{rd_1}|^2 + 1/\kappa} \tag{17}$$

Applying SIC operation, the received SINR for D1 is given by:

$$\gamma_{rd_1} \approx \frac{|h_{sr}|^2 |h_{rd_1}|^2 a_1 \psi}{|h_{rd_1}|^2 + 1/\kappa} \tag{18}$$

3. SYSTEM PERFORMANCE ANALYSIS

The outage probability (OP) of the destination node D2 can be given by:

$$\begin{aligned} OP_{D_2}^1 &= \Pr \left[\max(\gamma_{sd_2}, \gamma_{rd_2}) < \gamma_{02} \right] \\ &= \Pr(\gamma_{sd_2} < \gamma_{02}) \Pr(\gamma_{rd_2} < \gamma_{02}) \end{aligned} \tag{19}$$

Where $\gamma_{02} = 2^{2R_2} - 1$ with R_2 being the target rate at the D2. From (8), we have:

$$\begin{aligned}
\Pr(\gamma_{sd_2} < \gamma_{02}) &= \Pr\left(\frac{|h_{sd_2}|^2 a_2 \psi}{|h_{sd_2}|^2 a_1 \psi + 1} < \gamma_{02}\right) \\
&= \Pr\left(|h_{sd_2}|^2 \psi [a_2 - \gamma_{02} a_1] < \gamma_{02}\right) \\
&= \begin{cases} 1 - \exp\left(-\frac{\gamma_{02} \lambda_{sd_2}}{\psi [a_2 - \gamma_{02} a_1]}\right), & \text{if } a_2 > \gamma_{02} a_1 \\ 1, & \text{if } a_2 \leq \gamma_{02} a_1 \end{cases}
\end{aligned} \tag{20}$$

Where λ_{sd_2} is the mean of the random variable (RV) $|h_{sd_2}|^2$. From (16), we can calculate the second probability of (19)

$$\begin{aligned}
&\Pr(\gamma_{rd_2} < \gamma_{02}) \\
&= \Pr\left(\frac{|h_{sr}|^2 |h_{rd_2}|^2 a_2 \psi}{|h_{sr}|^2 |h_{rd_2}|^2 a_1 \psi + |h_{rd_2}|^2 + 1/\kappa} < \gamma_{02}\right) = \\
&\Pr\left(\frac{\varphi_1 \varphi_2 a_2 \psi}{\varphi_1 \varphi_2 a_1 \psi + \varphi_2 + 1/\kappa} < \gamma_{02}\right) = \\
&\Pr\left[\varphi_2 (\varphi_1 a_2 \psi - \gamma_{02} \varphi_1 a_1 \psi - \gamma_{02}) < \frac{\gamma_{02}}{\kappa}\right] = \\
&\int_0^g f_{\varphi_1} d\varphi_1 + \int_g^\infty \Pr\left(\varphi_2 < \frac{\gamma_{02}}{\kappa [\varphi_1 a_2 \psi - \gamma_{02} \varphi_1 a_1 \psi - \gamma_{02}]}\right) f_{\varphi_1} d\varphi_1 = \\
&1 - \lambda_{sr} \int_g^\infty \exp\left(-\frac{\gamma_{02} \lambda_{rd_2}}{\kappa [\varphi_1 a_2 \psi - \gamma_{02} \varphi_1 a_1 \psi - \gamma_{02}]}\right) \exp(-\lambda_{sr} \varphi_1) d\varphi_1
\end{aligned} \tag{21}$$

Where we denote $g = \frac{\gamma_{02}}{a_2 \psi - \gamma_{02} a_1 \psi}$, $\varphi_1 = |h_{sr}|^2$, $\varphi_2 = |h_{rd_2}|^2$, λ_{sr} and λ_{rd_2} are the mean of RV $|h_{sr}|^2, |h_{rd_2}|^2$, respectively.

By changing a variable $x = \varphi_1 a_2 \psi - \gamma_{02} \varphi_1 a_1 \psi - \gamma_{02} \Rightarrow \varphi_1 = \frac{\mathcal{G}(x + \gamma_{02})}{\gamma_{02}}$, (21) can be rewritten as:

$$\begin{aligned}
\Pr(\gamma_{rd_2} < \gamma_{02}) &= 1 - \frac{\lambda_{sr} \mathcal{G} \exp(-\lambda_{sr} \mathcal{G})}{\gamma_{02}} \\
&\int_0^\infty \exp\left(-\frac{\gamma_{02} \lambda_{rd_2}}{\kappa x}\right) \exp\left(-\frac{\lambda_{sr} x \mathcal{G}}{\gamma_{02}}\right) dx
\end{aligned} \tag{22}$$

Apply eq (3.324,1) of [15], (22) can be reformulated as:

$$\begin{aligned}
\Pr(\gamma_{rd_2} < \gamma_{02}) &= 1 - 2 \exp(-\lambda_{sr} \mathcal{G}) \\
&\times \sqrt{\frac{\lambda_{sr} \lambda_{rd_2} \mathcal{G}}{\kappa}} \times K_1\left(2\sqrt{\frac{\lambda_{sr} \lambda_{rd_2} \mathcal{G}}{\kappa}}\right)
\end{aligned} \tag{23}$$

Where $K_v(\bullet)$ is the modified Bessel function of the second kind and v^{th} order. Substituting (20) and (23) into (19), finally, we can obtain:

$$\begin{aligned}
OP_{D_2}^1 &= \left\{1 - \exp(-\lambda_{sd_2} \mathcal{G})\right\} \\
&\left\{1 - 2 \exp(-\lambda_{sr} \mathcal{G}) \times \sqrt{\frac{\lambda_{sr} \lambda_{rd_2} \mathcal{G}}{\kappa}} \times K_1\left(2\sqrt{\frac{\lambda_{sr} \lambda_{rd_2} \mathcal{G}}{\kappa}}\right)\right\}
\end{aligned} \tag{24}$$

Hence, the outage probability (OP) of the destination D₁ can be given by:

$$\begin{aligned}
 OP_{D_1}^l &= \Pr(\gamma_{sd_{21}} < \gamma_{02}, \gamma_{sd_1} < \gamma_{01}) \\
 &\times \Pr(\gamma_{rd_{21}} < \gamma_{02}, \gamma_{rd_1} < \gamma_{01}) \\
 &= \left[1 - \Pr(\gamma_{sd_{21}} \geq \gamma_{02}, \gamma_{sd_1} \geq \gamma_{01}) \right] \times \\
 &\left[1 - \Pr(\gamma_{rd_{21}} \geq \gamma_{02}, \gamma_{rd_1} \geq \gamma_{01}) \right] = P_1 \times P_2
 \end{aligned} \tag{25}$$

Where $P_1 = \left[1 - \Pr(\gamma_{sd_{21}} \geq \gamma_{02}, \gamma_{sd_1} \geq \gamma_{01}) \right]$, $P_2 = \left[1 - \Pr(\gamma_{rd_{21}} \geq \gamma_{02}, \gamma_{rd_1} \geq \gamma_{01}) \right]$. And $\gamma_{01} = 2^{2R_1} - 1$ with R₁ being the target rate at the D₁. From (10) and (11), P₁ can be calculated as:

$$\begin{aligned}
 P_1 &= \left[1 - \Pr \left(\frac{|h_{sd_1}|^2 a_2 \psi}{|h_{sd_1}|^2 a_1 \psi + 1} \geq \gamma_{02}, |h_{sd_1}|^2 a_1 \psi \geq \gamma_{01} \right) \right] \\
 &= 1 - \Pr \left(|h_{sd_1}|^2 \geq \frac{\gamma_{02}}{a_2 \psi - \gamma_{02} a_1 \psi}, |h_{sd_1}|^2 \geq \frac{\gamma_{01}}{a_1 \psi} \right) \\
 &= 1 - \Pr \left\{ |h_{sd_1}|^2 \geq \max \left[\frac{\gamma_{02}}{a_2 \psi - \gamma_{02} a_1 \psi}, \frac{\gamma_{01}}{a_1 \psi} \right] \right\} \\
 &= \Pr \left[|h_{sd_1}|^2 < \Xi \right] = 1 - \exp(-\lambda_{sd_1} \Xi)
 \end{aligned} \tag{26}$$

Where λ_{sd_1} is the mean of RV $|h_{sd_1}|^2$ and $\Xi = \max \left[\frac{\gamma_{02}}{a_2 \psi - \gamma_{02} a_1 \psi}, \frac{\gamma_{01}}{a_1 \psi} \right]$. From (17) and (18), P₂ can be calculated as:

$$\begin{aligned}
 P_2 &= 1 - \Pr \left\{ \frac{|h_{sr}|^2 |h_{rd_1}|^2 a_2 \psi}{|h_{sr}|^2 |h_{rd_1}|^2 a_1 \psi + |h_{rd_1}|^2 + 1/\kappa} \right. \\
 &\quad \left. \geq \gamma_{02}, \frac{|h_{sr}|^2 |h_{rd_1}|^2 a_1 \psi}{|h_{rd_1}|^2 + 1/\kappa} \geq \gamma_{01} \right\} \\
 &= 1 - \Pr \left\{ \varphi_3 \geq \frac{A/\kappa}{\varphi_1 - A}, \varphi_1 \geq A \right\} \\
 &\times \Pr \left\{ \varphi_3 \geq \frac{B/\kappa}{\varphi_1 - B}, \varphi_1 \geq B \right\} \\
 &= 1 - \Pr \left\{ \varphi_3 \geq \frac{\Xi/\kappa}{\varphi_1 - \Xi}, \varphi_1 \geq \Xi \right\} \\
 &= 1 - \int_{\Xi}^{\infty} f_{\varphi_1}(\varphi_1) d\varphi_1 \int_{\frac{\Xi/\kappa}{\varphi_1 - \Xi}}^{\infty} f_{\varphi_3}(\varphi_3) d\varphi_3 \\
 &= 1 - \int_{\Xi}^{\infty} \left[1 - F_{\varphi_3} \left(\frac{\Xi/\kappa}{\varphi_1 - \Xi} \right) \right] f_{\varphi_1}(\varphi_1) d\varphi_1 \\
 &= 1 - \lambda_{sr} \int_{\Xi}^{\infty} \exp \left[-\frac{\lambda_{rd_1}(\Xi/\kappa)}{\varphi_1 - \Xi} \right] \exp(-\lambda_{sr} \varphi_1) d\varphi_1
 \end{aligned} \tag{27}$$

Where $\varphi_1 = |h_{sr}|^2, \varphi_3 = |h_{rd_1}|^2$,
 $A = \frac{\gamma_{02}}{a_2\psi - \gamma_{02}a_1\psi}, B = \frac{\gamma_{01}}{a_1\psi}, \Xi = \max(A, B)$. And $\lambda_{sr}, \lambda_{rd_1}$ are the mean of RV $|h_{sr}|^2, |h_{rd_1}|^2$,

respectively changing variable $y = \varphi_1 - \Xi$, (27) can be rewritten as:

$$P_2 = 1 - \lambda_{sr} \int_0^\infty \exp\left(-\frac{\lambda_{rd_1}\Xi}{\kappa y}\right) \exp[-\lambda_{sr}(y + \Xi)] dy$$

$$= 1 - \lambda_{sr} \exp(-\lambda_{sr}\Xi) \int_0^\infty \exp\left(-\frac{\lambda_{rd_1}\Xi}{\kappa y} - \lambda_{sr}y\right) dy$$
(28)

Apply equation (3.324,1) of [table of integral], (22) can be reformulated as:

$$P_2 = 1 - 2\exp(-\lambda_{sr}\Xi) \times \sqrt{\frac{\lambda_{sr}\lambda_{rd_1}\Xi}{\kappa}} \times K_1\left(2\sqrt{\frac{\lambda_{sr}\lambda_{rd_1}\Xi}{\kappa}}\right)$$
(29)

where $K_v(\bullet)$ is the modified Bessel function of the second kind and v^{th} order. Substituting (26) and (29) into (25), finally, the outage probability of D_1 can be claimed as:

$$OP_{D_1}^1 = \left[1 - \exp(-\lambda_{sd_1}\Xi)\right]$$

$$\left[1 - 2\exp(-\lambda_{sr}\Xi) \times \sqrt{\frac{\lambda_{sr}\lambda_{rd_1}\Xi}{\kappa}} \times K_1\left(2\sqrt{\frac{\lambda_{sr}\lambda_{rd_1}\Xi}{\kappa}}\right)\right]$$
(30)

4. NUMERICAL RESULTS AND DISCUSSION

In this section, we investigate the OP of the model system using Monte Carlo simulation in connection with the primary system parameters [16-26]. In Figure 3, the effect of a_2 on the system OP is plotted with the primary system parameters as $\eta=0.8, R_1=R_2=0.25, 0.5$ bps/Hz, $\alpha=0.5$. From the results, we can see that the OP of the destination D_1 significantly decreases with the rising of a_2 . However, the OP of the D_2 decreases when a_2 increases from 0.55 to 0.7 and after that has a massive increase with the remaining values of a_2 . In the same way, the system OP versus α is drawn in Figure 4. In this simulation, we set $\eta=0.8, R_1=R_2=0.5$ bps/Hz, $P_S/N_0=0.5$, and $a_2=0.7, 0.9$. As shown in Figure 4, we can state that the OP of the model system has a slight decrease when α varies from 0 to 1. In both Figures 3 and 4, the simulation and analytical results are the same with all values of α and a_2 .

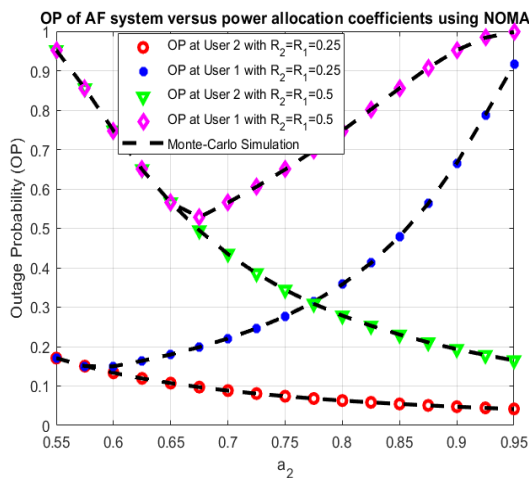


Figure 3. OP versus a_2

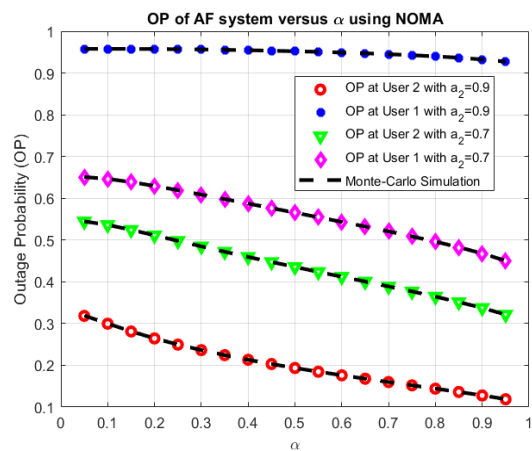
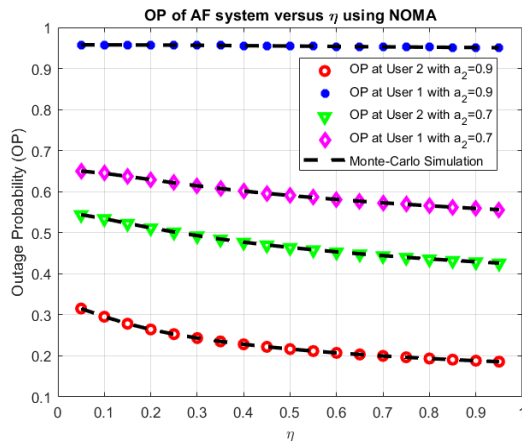
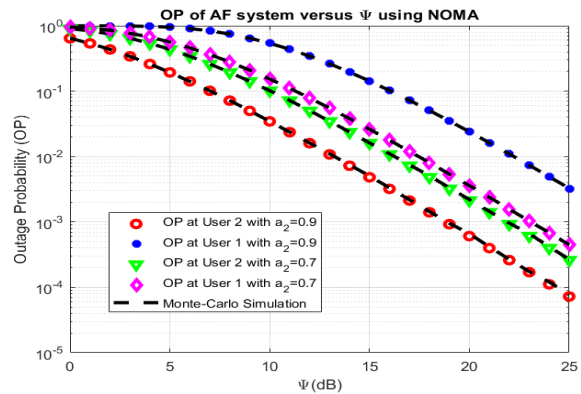


Figure 4. OP versus α

Furthermore, we investigate the effect of η and ψ on the OP of the model system as plotted in Figures 5 and 6. In these Figures, we set the primary parameters as $a_2=0.7, 0.9, R_1=R_2=0.5$ bps/Hz, $P_s/N_0=0.5$. From Figures 5 and 6, it can be observed that the system OP has a slight decrease when η varies from 0 to 1 and the system OP crucially decreases with the rising of ψ from 0 to 25. In all two Figures, the analytical and simulation results agree well with each other. On another hand, the comparison of the system OP of two destination nodes is demonstrated in all Figures. From the results, we can state that the system OP of the destination node D_2 is better than the destination node D_1 .

Figure 5. OP versus η Figure 6. OP versus ψ

5. CONCLUSION

In this research, we propose EH NOMA network system over the Rayleigh fading channel using selection combining at the receiver. The closed-form expression of the OP of the model system by Monte Carlo simulation is derived. Moreover, the comparison of the OP of two destination users is investigated in connection with the primary system parameters. From the results, we can see that all the analytical and simulation results are the same with the primary system parameters using Monte Carlo simulation. These results can be provided a novel recommendation for improving the performance of the EH NOMA communication network system.

ACKNOWLEDGEMENTS

This research was supported by National Key Laboratory of Digital Control and System Engineering (DCSELAB), HCMUT, VNU-HCM, Vietnam.

REFERENCES

- [1] H. Chen, C. Zhai, Y. Li and B. Vucetic, "Cooperative strategies for wireless-powered communications: An overview," in *IEEE Wireless Communications*, vol. 25, no. 4, pp. 112-119, August 2018.
- [2] Yu, H., Lee, H., & H. Jeon, "What is 5G? Emerging 5G mobile services and network requirements," in *5G Mobile Services and Scenarios: Challenges and Solutions*, vol. 9, pp. 1848, 2017.
- [3] V. Sharma and P. Karmakar, "A novel method of opportunistic wireless energy harvesting in cognitive radio networks," in *2015 7th International Conference on Computational Intelligence, Communication Systems and Networks*, Riga, 2015, pp. 59-64, 2015.
- [4] F. Boccardi, R. W. Heath, A. Lozano, T. L. Marzetta and P. Popovski, "Five disruptive technology directions for 5G," in *IEEE Communications Magazine*, vol. 52, no. 2, pp. 74-80, February 2014.
- [5] L. Dai, B. Wang, Y. Yuan, S. Han, C. I and Z. Wang, "Non-orthogonal multiple access for 5G: solutions, challenges, opportunities, and future research trends," in *IEEE Communications Magazine*, vol. 53, no. 9, pp. 74-81, Sep 2015.
- [6] Y. Saito, Y. Kishiyama, A. Benjebbour, T. Nakamura, A. Li and K. Higuchi, "Non-Orthogonal Multiple Access (NOMA) for cellular future radio access," in *2013 IEEE 77th Vehicular Technology Conference (VTC Spring)*, Dresden, pp. 1-5, 2013.
- [7] Z. Ding, P. Fan and H. V. Poor, "Impact of user pairing on 5G Nonorthogonal multiple-access downlink transmissions," in *IEEE Transactions on Vehicular Technology*, vol. 65, no. 8, pp. 6010-6023, Aug 2016.

- [8] S. Timotheou and I. Krikidis, "Fairness for Non-Orthogonal Multiple Access in 5G Systems," in *IEEE Signal Processing in Letters*, vol. 22, no. 10, pp. 1647-1651, Oct. 2015.
- [9] Al-Imari, Mohammed, Pei Xiao, Muhammad Ali Imran, and Rahim Tafazolli, "Uplink Non-orthogonal multiple access for 5G wireless networks," in *2014 11th International Symposium on Wireless Communications Systems (ISWCS)*, pp.781-785, 2014.
- [10] J. Kim and I. Lee, "Non-Orthogonal multiple access in coordinated direct and relay transmission," in *IEEE Communications Letters*, vol. 19, no. 11, pp. 2037-2040, Nov 2015.
- [11] M. Xu, F. Ji, M. Wen and W. Duan, "Novel receiver design for the cooperative relaying system with Non-Orthogonal multiple access," in *IEEE Communications Letters*, vol. 20, no. 8, pp. 1679-1682, Aug 2016.
- [12] Kizilirmak, Refik Caglar, "Non-Orthogonal Multiple Access (NOMA) for 5G networks," in *Towards 5G Wireless Networks-A Physical Layer Perspective*, 2016.
- [13] Y. Liu, Z. Ding, M. ElKashlan and H. V. Poor, "Cooperative Non-orthogonal multiple access with simultaneous wireless information and power transfer," in *IEEE Journal on Selected Areas in Communications*, vol. 34, no. 4, pp. 938-953, April 2016.
- [14] Z. Ding, Z. Yang, P. Fan and H. V. Poor, "On the performance of Non-orthogonal multiple access in 5G systems with randomly deployed users," in *IEEE Signal Processing Letters*, vol. 21, no. 12, pp. 1501-1505, Dec 2014.
- [15] Daniel Zwillinger and Victor Moll. "Table of integrals, series, and products," in Academic Press, 2014.
- [16] Tan N. Nguyen, T. H. Q. Minh, Phuong T. Tran and Miroslav Voznak, "Adaptive energy harvesting relaying protocol for two-way half duplex system network over Rician Fading channel," in *Wireless Communications and Mobile Computing*, 2018.
- [17] T. Nguyen, T. Quang Minh, P. Tran, M. Vozňák, "Energy harvesting over Rician Fading channel: A performance analysis for half-duplex bidirectional sensor networks under hardware impairments," in *Sensors*, vol. 18, pp. 1781, 2018.
- [18] Tan N. Nguyen, T. H. Q. Minh, Phuong T. Tran, Miroslav Voznak, T. T. Duy, Thanh-Long Nguyen and Phu Tran Tin, "Performance enhancement for energy harvesting based two-way relay protocols in wireless Ad-hoc networks with partial and full relay selection methods," in *Ad hoc networks*, vol 84, pp. 178-187, 2019.
- [19] T. N. Nguyen, T. H. Q. Minh, T.-L. Nguyen, D.-H. Ha, M. Voznak, "Performance analysis of user selection protocol in cooperative networks with power splitting protocol based energy harvesting o Energy harvesting over Rician Fading channel: A performance analysis for half-duplex Bidirectional Sensor Networks under Hardware Impairments ver Nakagami-m/Rayleigh channel," in *Electronics*, vol. 8, pp. 448, 2019.
- [20] T. N. Nguyen, T. H. Q. Minh, T.-L. Nguyen, D.-H. Ha, M. Voznak, "Multi-Source power splitting energy harvesting relaying network in half-duplex system over block Rayleigh Fading channel: System performance analysis," in *Electronics*, vol. 8, pp. 67, 2019.
- [21] F. De Rango and M. Tropea, "Energy saving and load balancing in wireless ad hoc networks through ant-based routing," in *2009 International Symposium on Performance Evaluation of Computer & Telecommunication Systems*, Istanbul, pp. 117-124, 2009.
- [22] F. De Rango, & M. Tropea, "Swarm intelligence based energy saving and load balancing in wireless ad hoc networks," in *In Proceedings of the 2009 workshop on Bio-inspired algorithms for distributed systems*, ACM, pp. 77-84, June 2009.
- [23] M. Tropea and P. Fazio, "A new threshold switching scheme for a DVB-RCS+M return link in a terrestrial scenario," in *2012 25th IEEE Canadian Conference on Electrical and Computer Engineering (CCECE)*, Montreal, QC, pp. 1-4, 2012.
- [24] M. Tropea, F. Veltri, F. De Rango, A. Santamaria and L. Belcastro, "Two step based QoS scheduler for DVB-S2 satellite system," in *2011 IEEE International Conference on Communications (ICC)*, Kyoto, pp. 1-5, 2011.
- [25] Tin, Phu Tran, Le Anh Vu, Tan N. Nguyen, and Thanh-Long Nguyen, "User selection protocol in DF cooperative networks with Hybrid TSR-PSR protocol based full-duplex energy harvesting over Rayleigh Fading channel: System performance analysis," in *Indonesian Journal of Electrical Engineering and Computer Science*, vol. 3, no. 2, pp. 534-542, 2019.
- [26] Tin, Phu Tran, Minh Tran, Tan N. Nguyen, and Thanh-Long Nguyen, "System performance analysis of Hybrid time-power switching protocol of EH bidirectional relaying network in amplify-and-forward mode," in *Indonesian Journal of Electrical Engineering and Computer Science*, vol. 14, no. 1, pp. 123-131, 2019.